THE EFFECT OF ELECTRICAL AND MECHANICAL ANTENNA DOWN-TILTING IN UMTS NETWORKS

I. Forkel[1], A. Kemper[1], R. Pabst[1], R. Hermans[2]
[1]Communication Networks, Aachen University of Technology, Germany
[2]Libertel-Vodafone, Maastricht, Netherlands

***Abstract*— In an interference-limited CDMA system, network planning and the optimal installation of infrastructure components are important issues. This is not only to increase system capacity but also to allow for a smooth network operation. Whereas the Node B locations can hardly be changed, modern antennas provide adaptation mechanisms with which the antenna down-tilt angle can be adapted to the various needs of the network. This is dependent on the locations of the base station sites, the resulting cell sizes, and the current traffic situations. The simulations presented in this paper show basic effects on network coverage and capacity due to changes in the antenna down-tilt angle configuration. It is differed between mechanical and electrical adjustment of the down-tilt resulting in slightly different antenna characteristics.**

***Keywords*—UMTS, Antenna, Network Capacity, Quality of Service, W-CDMA**

I. Introduction

With the introduction of *Universal Mobile Telecommunications System* (UMTS) and its *Code Division Multiple Access* (CDMA) technology, a lot of research focus on the capacity of those 3rd generation mobile communication networks [1, 2]. As already implemented in 2nd generation *Global System for Mobile* (GSM), base station sites are equipped with sectored antennas. Whereas in GSM adjacent sector interference could be neglected due to sufficient carrier spacing, UMTS will re-use the same carrier frequency in every sector of a Node B base station. Resulting from such a frequency re-use factor of one, the problem of overlapping sector interference arises. This additional interference results in varying network capacity and coverage depending on the antenna down-tilt. Furthermore, the way this down-tilt is realized—either in a mechanical way or in an electrical manner—influences the interference experienced in a neighbouring sector.

This research evaluates network performance in a single site scenario divided into three sectors examining different antenna down-tilt angles and traffic conditions. The paper is organized as follows. The next Sec. II describes the type of antenna commonly used in UMTS networks and its installation. In Sec. III the simulated scenario and relevant radio parameters are introduced. Sec. IV contains the results obtained by dynamic simulation. Finally, Sec. V concludes the paper.

II. The UMTS Antenna

At the Node B, the KATHREIN 741784 antenna [3] can be used. It provides an additional antenna gain in the direction of its main beam of approximately 18 dBi against an isotropic radiating antenna. Beneath this gain an individual antenna pattern can be obtained. This pattern gives additional attenuation values with respect to the direction of an emitted radio wave. Fig. 1 illustrates the antenna characteristic versus azimuth (vertical) angle θ and elongation (horizontal) angle ϕ for this type of antenna. Within this antenna pattern typical deep fades are noticeable. They result from the antenna construction out of several single antenna segments. Such a surface mounting leads to constructive and destructive interference of the electro-magnetic waves originated from the single antenna segments. The fades may reach an attenuation of up to -60 dB.

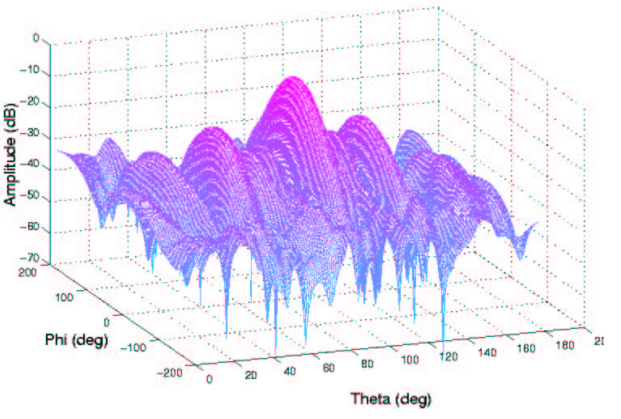

Fig. 1. Node B antenna characteristic

For the adjustment of the antenna down-tilt angle ϑ, two different mechanisms are available. Either the antenna can be tilted as a whole or single segments of the antenna surface can virtually be shifted against each other. The first means a mechanical down-tilting of the complete antenna including all its segments as illustrated in Fig. 2. The second method is realized by adjusting the phase of the control signals to the different segments electrically. As a result, the virtual distance between the antenna back plate and each single segment varies so that an apparently tilted surface of the antenna front plate is resulting. Fig. 3 depicts the method of electrical antenna down-tilting.

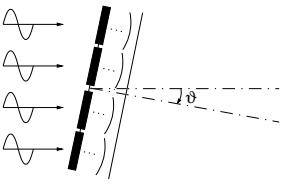

Fig. 2. Mechanical down-tilt

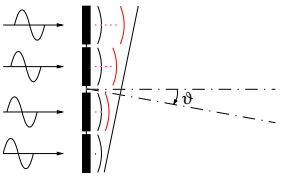

Fig. 3. Electrical down-tilt

As a result, the antenna characteristic changes slightly if the electrical way of adjusting the antenna down-tilt is chosen. Since the virtual distance of the separate antenna segments to each other vary depending on the electrical down-tilt angle ϑ, the fading caused by destructive inter-

ference of electro-magnetic waves originating from the single segments is also shifted. Such an effect causes the antenna characteristic to vary depending on the chosen angle ϑ. Unlike the electrical down-tilt adaptation, the antenna characteristic is not affected if the down-tilt is varied in a mechanical way.

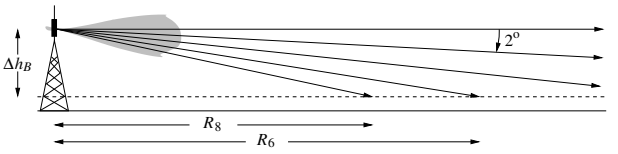

Fig. 4. Antenna down-tilt angles and cell radii

Mechanical and electrical down-tilts of the antenna are investigated in this paper. The angle ϑ is varied between two and eight degree. Fig. 4 illustrates the antenna settings in our simulation. Depending on the chosen down-tilt, a geometric cell radius $R_\vartheta = \Delta h_B / \tan\vartheta$ can be estimated where the main beam hits the ground.

III. Simulation Scenario

The simulation scenario is a squared area with size 1 500 m×1 500 m resulting in a simulation area of 2.25 km^2. One *Base Station* (BS) site is placed in the center of this area. This BS represents three Node B, each spanning a single 120° sectored cell. The maximum Node B to *User Equipment* (UE) separation is therefore 1061 m. Fig. 5 illustrates the geometric settings of this initial simulation scenario.

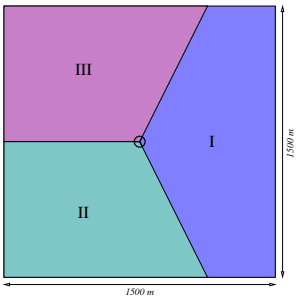

Fig. 5. Single site scenario

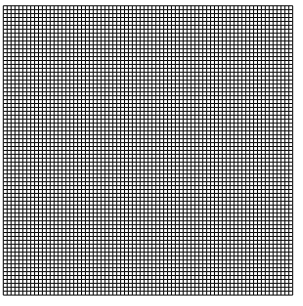

Fig. 6. Road map of the scenario

The BS antenna height is 25 m, all UE is set at a height of 1.5 m. The height difference is an important parameter when the system behavior with different antenna down-tilt angles is to be investigated. With the scenario size as mentioned above and a constant height difference of 23.5 m, the azimuth angle ranges from 1.27° to 90.0°. The smallest angle belongs to a UE located at a scenario corner. The biggest will be the case in which a UE is placed at the BS location directly below it.

In order to model homogeneously distributed users, a road map with a high resolution is included in this scenario, which will provide measurements for any location on a 20 m spaced grid structure. This so-called road map is illustrated in Fig. 6. Mobile users travel along the roads. When arriving at intersections, any possible further direction is chosen with equal probability. Within this model, a total length of all streets of 150×1480 m=222 km is given in the scenario. The mobile speed for the speech users is set to 30 km/h.

TABLE I
Radio parameters of the simulation

UL frequency	1920–1925 MHz
DL frequency	2110–2115 MHz
Bandwidth	5 MHz
Radio frame duration	10 ms
Spreading factor UL	64
Spreading factor DL	128
Code (un-)orthogonality UL	1.0
Code (un-)orthogonality DL	0.3
CIR target UL /DL	−17.75 dB

Tab. I summarizes the basic radio specific parameters concerning the physical layer settings and conditions. Frequency range is considered at one of the possible bands auctioned in Europe. The remaining parameters are taken from the UMTS standard [4].

The propagation model is based on the proposal in [5], which is a modified Hata-Okumura model, adapted for UMTS purposes. Pathloss in dB is calculated by the expression

$$L = 124.6 + 36.2 \log\left(\frac{R}{[\text{km}]}\right), \qquad (1)$$

where R is the distance between the transmitting and receiving antenna. An average carrier frequency of f=2 GHz and a height difference between UE and Node B antenna of Δh_B=23.5 m are considered.

Traffic is chosen to be 12.2 kbps speech with 50 % service activity. On the physical layer this service requires one code with spreading factor 128 in *Downlink* (DL) and one with spreading factor 64 in *Uplink* (UL) in parallel. Theoretically, DL capacity is limited to 125 Erlang per cell since the other codes are needed for signaling purposes. UL capacity is not restricted by physical radio resources as a user specific scrambling code is assigned in addition to the *Orthogonal Variable Spreading Factor* (OVSF) code (which are limited). As a result, UL signals are uncorrelated and interfere with each other. This is considered by using an (un-)orthogonality factor of 1.0. In DL, intra-cell interference from other user's codes is multiplied with a factor of 0.3 with respect to the orthogonality of the OVSF codes. The target *Carrier to Interference Ratio* (CIR) for the inner loop power control is set to −17.75 dB according to [6]. Simulations are performed with traffic varying between 80 and 120 Erlang, which means 80 to 100 speech users per sector.

IV. Simulation Results

The coverage area evaluation is made with consideration of the DL CIR and UL transmitting power. An area pixel is covered if the average DL CIR in this pixel is above the required target of −17.75 dB and the mean UL transmitting power is not higher than 24 dBm (which means 3 dB below UE's maximum transmitting power). Because of the high DL transmitting power available and negligible inter-cell interference in this scenario, the first criterion can easily be achieved except for some locations directly beneath the Node B antenna. On the other

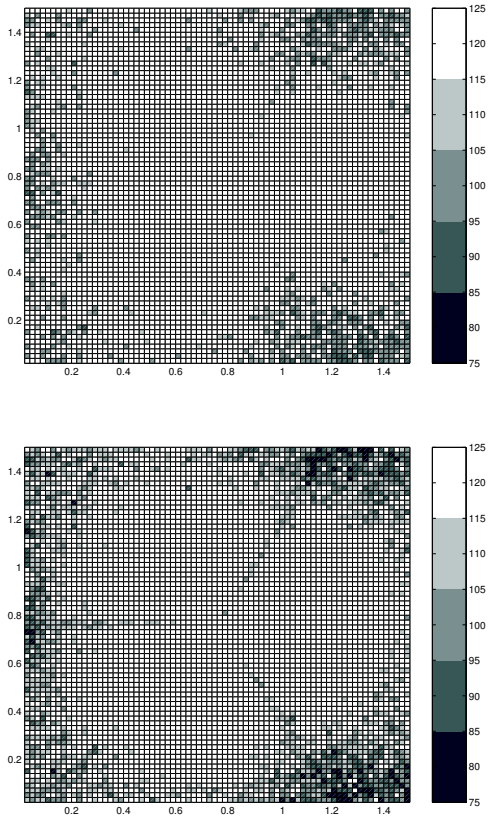

Fig. 7. Coverage area for mechanical antenna down-tilt of 2° and 8°

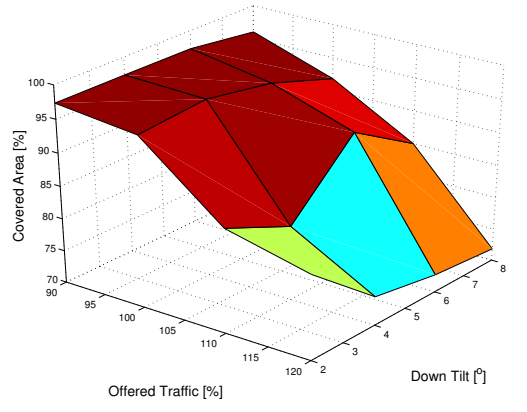

Fig. 8. Percentage of covered area with respect to offered traffic and mechanical antenna down-tilt

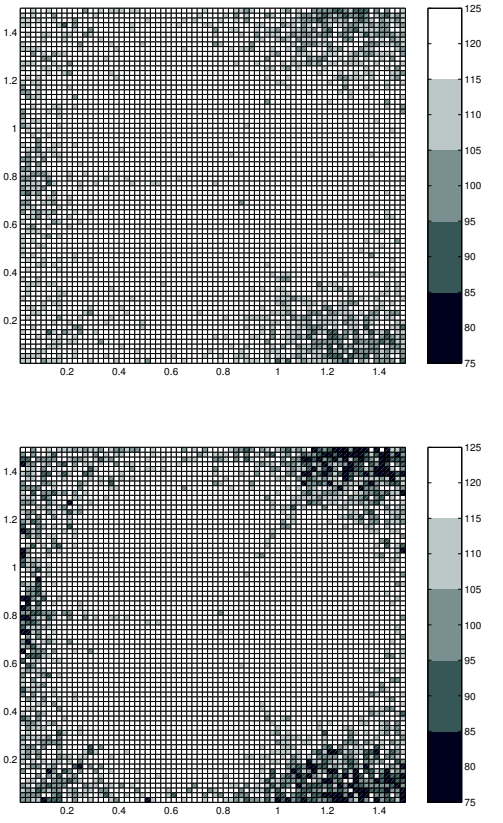

Fig. 9. Coverage area for electrical antenna down-tilt of 2° and 8°

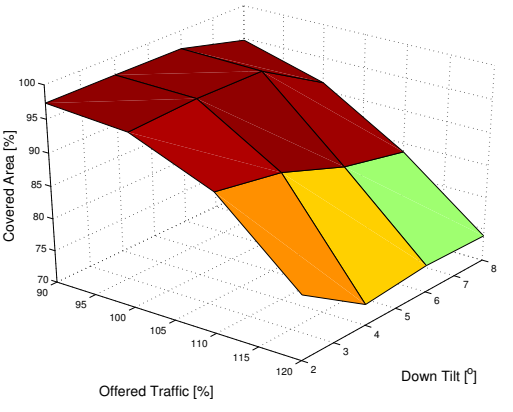

Fig. 10. Percentage of covered area with respect to offered traffic and electrical antenna down-tilt

hand, the UL transmitting power evaluation is a worst case estimation of the coverage area. The UE's available transmitting power range is limited to a maximum of 27 dBm. Particularly when the available antenna gain at the Node B is low, the connection quality, i.e. the CIR, is getting worse causing the power control to increase the transmitting power to its maximum.

The effect of cell breathing can be observed, independent from the selected antenna down-tilt. Cell breathing means that the higher the traffic per sector the smaller the coverage area. In other words, as the offered traffic increases, the covered area decreases. The strongest impact of the cell breath can be determined at locations far from the Node B but also in the area of adjacent sectors. Fig. 7 and Fig. 9 illustrate the cell breathing for mechanical and electrical down-tilts of 2° and 8°. For smaller antenna down-tilts and low traffic, almost the whole scenario area is covered. It can be seen that the coverage ratio for the mechanical and electrical case are very similar. Comparing the coverage maps for both cases at the same down-tilt angle, a slight advantage for the electrical down-tilt can be recognized.

The overall percentage of covered area with respect to the offered traffic and the down-tilt angles is depicted in

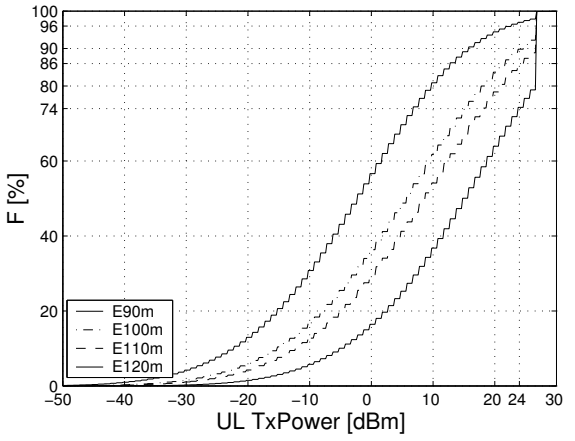

Fig. 11. UL transmitting power distribution (6° mechanical down-tilt)

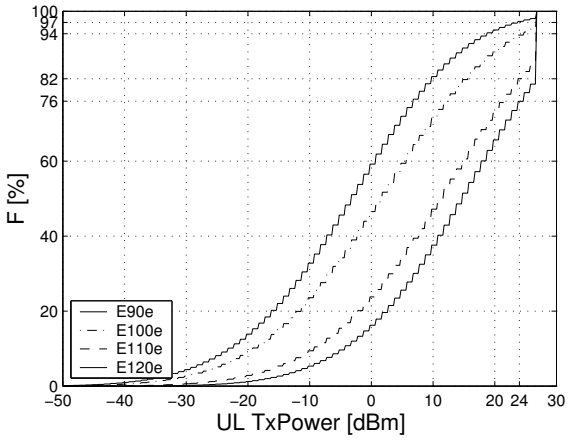

Fig. 12. UL transmitting power distribution (6° electrical down-tilt)

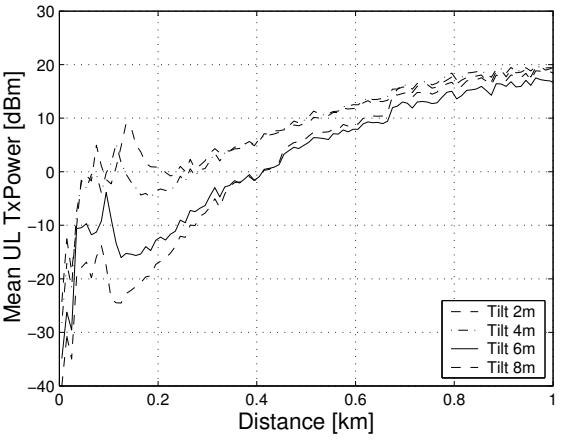

Fig. 13. UL transmitting power over distance with mechanical tilt

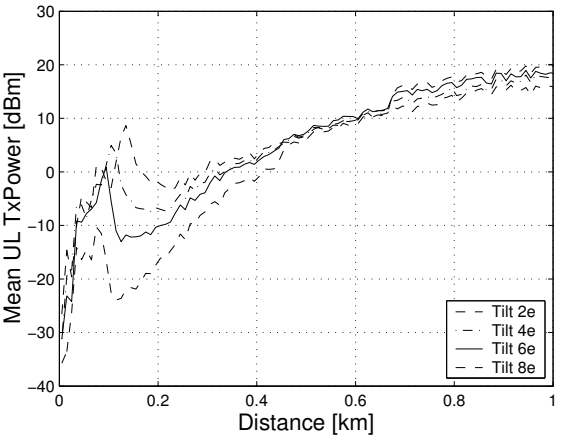

Fig. 14. UL transmitting power over distance with electrical tilt

Fig. 8 and Fig. 10 for the mechanical and electrical adjustment, respectively. The best performance is achieved at a mechanical down-tilt of 6°, especially if an offered traffic of 110 Erlang is considered. Nevertheless, there is a tendency that the lower the traffic the better a minor down-tilt angle performs—except at the high traffic of 120 Erlang. The mechanical down-tilt evaluation astonishes with a deep hole at offered traffic of 110 Erlang and 4° antenna down-tilt. This seems to be a worst case setup of the Node B antenna since all the evaluations are based on the same propagation model and differ only in the antenna patterns.

In Fig. 11 and Fig. 12, the UL transmitting power distribution functions at a constant down-tilt of 6° are presented. Depending on the offered traffic, approximately 2 % to 20 % of the connections for the mechanical case operate with the maximum transmitting power of 27 dBm, and 1 % to 19 % for electrical down-tilt, respectively. The outage level of 24 dBm is exceeded for even more measurements. At 120 Erlang, only up to 74 % of the values fulfill the coverage criterion with mechanical down-tilt, 76 % apply for electrical down-tilt.

In Fig. 13 and Fig. 14, the mean UL transmitting power at 110 Erlang versus the BS-UE separation is presented. The influence of the antenna inclination can clearly be observed. The more the antenna is angled, i.e. the larger the angle ϑ, the better is the radio provisioning at close distance and the worse the coverage at the cell border. With mechanical adjustment, the lowest mean transmitting power values are achieved with a down-tilt of 8° for cells smaller than 400 m and with 6° for larger cells up to 1 km. In case of an electrical antenna down-tilt, 8° performs best up to 550 m. For greater cell radii, an angle of 2° seems best since all the curves in Fig. 14 cross each other in the same range between 500 and 600 m. Nevertheless, smaller cells might even better be covered with down-tilt angles larger than 8°.

Fig. 15 and Fig. 18 contain the evaluation of mean CIR values with respect to the distance between UE and Node B at a constant load of 110 Erlang for different down-tilt angles. For distances below 250 m, the influence of the antenna pattern's first minimum and maximum, respectively, on the performance parameters can be observed. The effect on the curves is stronger for mechanical down-tilt and decreases with increasing down-tilt angle. Comparing the performance for mechanical and electrical down-tilt, it can be noticed that electrical adjustment shows advantageous CIR values and less variation.

In DL direction, the run of the curves for down-tilts below or equal 6° is rather constant at a mean CIR of -13.5 dB due to the relatively high lower bound of the

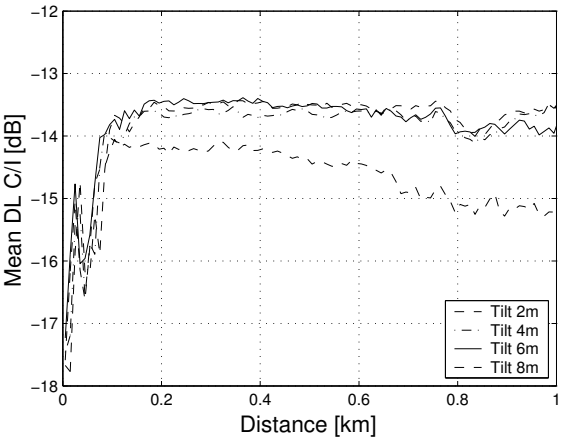

Fig. 15. Mean DL CIR over distance with mechanical tilt

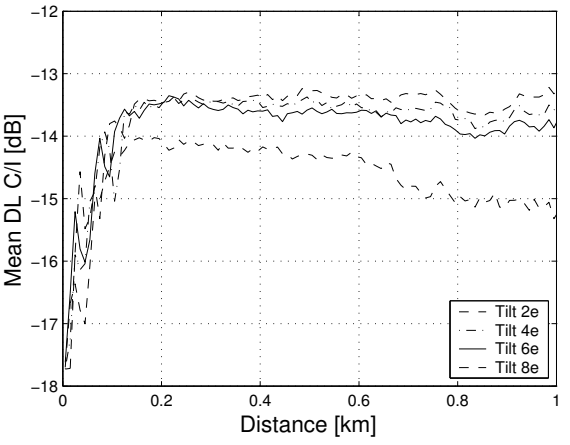

Fig. 16. Mean DL CIR over distance with electrical tilt

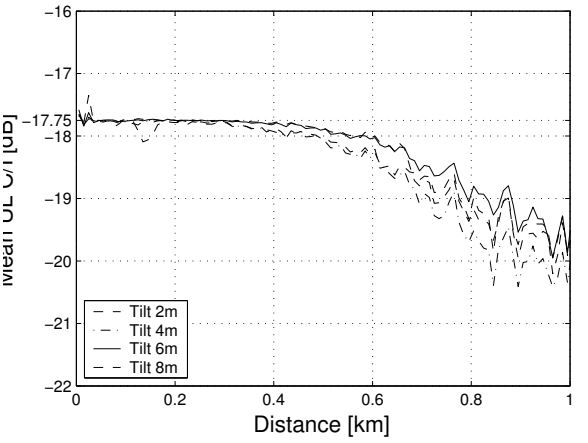

Fig. 17. Mean UL CIR over distance with mechanical tilt

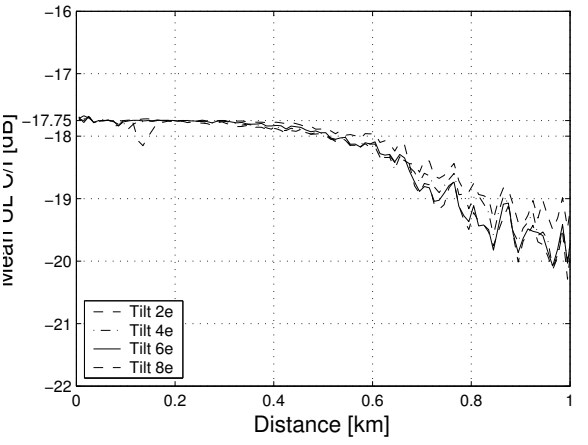

Fig. 18. Mean UL CIR over distance with electrical tilt

Node B's transmitting power. Lower CIR values are observed at close distances to the Node B because the antenna is emitting its power more to the cell border, i.e. it sends atop the UE. Although the performance of the 8° curve is worse, the CIR target is still overcome.

In UL, the curves run nearly constant, close to the required CIR target of -17.75 dB. Due to the influence of the antenna characteristic, the 2° curve even runs below the required threshold at a distance 120 m to 170 m from Node B. With greater distance to Node B, the UE's transmitting power can not further be increased. If the UE's maximum transmitting power is reached, the required threshold can not longer be met and the cell border for this down-tilt angle is reached. Evaluating the diagram for mechanical down-tilt, it can be recognized that the curves at 2° and 4° run below the CIR target already at 300 m distance, while the 6° and 8° curves run below the threshold later at 400 m.

V. Conclusion

Mechanical and electrical settings of the Node B's antenna down-tilt in a single site scenario with three sectors are discussed. Concerning the percentage of covered area under certain circumstances, the electrical adjustment of the down-tilt angle performs slightly better. An adaptation of the antenna settings to the expected traffic distribution and cell size is recommended anyway. Basically, the rule applies that the smaller the cell size the larger the antenna down-tilt, and the higher the traffic load per cell the smaller the antenna down-tilt should be.

Acknowledgment

The authors would like to thank Prof. B. Walke and S. Teerling of ComNets for their support and friendly advice to this work. The contributions of Libertel-Vodafone, especially B. Wouters, S. Moutarazak, and B. Haverkamp are highly appreciated.

References

[1] H. Holma and A. Toskala, *WCDMA for UMTS*, John Wiley & Sons, Chichester, UK, 2001.

[2] B. Walke, *Mobile Radio Networks*, John Wiley & Sons, Chichester, UK, 2001.

[3] Kathrein, "790 – 2200 MHz Base Station Antennas for Mobile Communications," 2001, Catalogue.

[4] 3GPP, "Technical Specification 25.211, Physical Channels and Mapping of Transport Channels onto Physical Channels (FDD)," Tech. Rep., 3rd Generation Partnership Project, June 2000.

[5] ETSI, "TR 101 112, Selection Procedures for the Choice of Radio Transmission Technologies of the UMTS (UMTS 30.03)," Tech. Rep., European Telecommunications Standards Institute, Apr. 1998.

[6] I. Forkel, P. Seidenberg, R. Pabst, and G. Heidelberger, "Performance Evaluation of Power Control Algorithms in Cellular UTRA Systems," in *Second Int. Conference on 3G Mobile Communication Technologies*, London, UK, Mar. 2001.